Impact of Thermohaline Variability on Sea Level Changes in the Southern Ocean

Marlen Kolbe[1,2], Fabien Roquet[2], Etienne Pauthenet[3], David Nerini[4]

[1]Faculty of Science and Engineering, University of Groningen, Groningen, The Netherlands
[2]Department of Marine Sciences, University of Gothenburg, Gothenburg, Sweden
[3]Sorbonne University, UPMC Univ., Paris 06, UMR 7159, LOCEAN-IPSL F-75005, Paris, France
[4]Aix-Marseille University, CNRS/INSU, University de Toulon, IRD, Mediterranean Institute of Oceanology (MIO) UM 110, Marseille, France

Key Points:

- Variability of vertical thermohaline modes induces regional patterns in steric height trends in the Southern Ocean.
- Steric height has risen north of the Polar Front and fallen south of it due to both thermo- and halosteric changes.
- The halosteric effect in the Southern Ocean is nowhere negligible and significantly reduces the rate of sea level rise around Antarctica.

Corresponding author: Marlen Kolbe, `m.kolbe@rug.nl`

Abstract

The Southern Ocean is responsible for the majority of the global oceanic heat uptake that contributes to global sea level rise. At the same time, ocean temperatures do not change at the same rate in all regions and sea level variability is also affected by changes in salinity. This study investigates ten years of steric height variability (2008 to 2017) in the Southern Ocean (30°S to 70°S) by analysing temperature and salinity variations obtained from the GLORYS-031 model provided by the European Copernicus Marine Environment Monitoring Service (CMEMS). The thermohaline variability is decomposed into thermohaline modes using a functional Principal Component Analysis (fPCA). Thermohaline modes provide a natural basis to decompose the joint temperature-salinity vertical profiles into a sum of vertical modes weighted by their respective principal components (PCs) that can be related to steric height. Interannual steric height trends are found to differ significantly between subtropical and subpolar regions, simultaneously with a shift from a thermohaline stratification dominated by the first 'thermal' mode in the north to the second 'saline' mode in the South. The Polar Front appears as a natural boundary between the two regions, where steric height variations are minimized. Despite higher melt rates and atmospheric temperatures, steric height in Antarctic waters (0-2000 m) has dropped since 2008 due to higher salt content in the surface and upper intermediate layer and partially colder waters, while subtropical waters farther north have mostly risen due to increased heat storage.

Plain Language Summary

Sea level variations on longer timescales mainly arise from mass changes or the thermo- and halosteric effects of temperature and salinity on water density. Recent variability in steric height in the Southern Ocean was investigated from 2008 to 2017 by analysing potential temperature and salinity variations obtained from a global ocean reanalysis. The work was performed using a functional approach to a standard Principal Component Analysis that was applied on vertical temperature and salinity profiles (2000 m). The resulting thermohaline modes contain information about the general temperature and salinity structure and their variations can be attributed to steric height changes. The results have shown that Antarctic waters above 2000 m have dropped since 2008 due to higher salt content and colder waters, while subtropical waters farther north have mostly risen due to increased heat storage. Those spatial differences in recent steric height trends also display on the total sea level rise (SLR) observed from satellite data, which shows a significantly higher rate of SLR in subtropical waters compared to higher latitudes of the Southern Ocean.

1 Introduction

There is still insufficient understanding of processes controlling sea level variability (SLV) in the Southern Ocean. Mostly due to sparse data and its dynamic complexity, the Southern Ocean remains one of the least understood oceans. What is presently known is that it takes up the vast majority (72% ± 28%) of the global atmospheric heat content (Frölicher et al., 2015; Armour et al., 2016; Shi et al., 2018) and that Southern Ocean waters above 2000 m depth were responsible for 35%–43% of the increase in the global Ocean Heat Content (OHC) from 1970 to 2017 (Meredith et al., 2019; Cheng et al., 2020). Studies have shown that this increase in heat uptake over the last four decades does not result in a uniform distribution of increased ocean temperature. Instead, waters north of the Antarctic Circumpolar Current (ACC) and especially at the surface show significant warming, whilst south of the ACC there is very little warming so far. Although this delayed warming effect close to the coast has already been detected by previous studies, there is no scientific consensus regarding

the actual cause(s) for this observation (Goosse et al., 2004; Li et al., 2013; Sallée et al., 2013; Armour et al., 2016).

Armour et al. (2016) have suggested that the dominant cause for this delayed warming trend lies in the dynamics of the meridional overturning circulation (MOC). Although the vast majority of oceanic heat uptake occurs in higher latitudes of the Southern Ocean, those areas simultaneously present those with the least amount of heat stored. The authors concluded that instead of heat being stored locally, the residual mean flow (upwelling waters along the ACC flowing equatorward) transports the absorbed heat to waters farther north. Following earlier studies, Armour et al. (2016) further noted that the strengthening and poleward shift of winds contributed to the past and present cooling of Antarctic waters through enhanced advection of cool high-latitude surface waters (Oke & England, 2004). Other explanations include a meltwater-induced freshening of waters close to Antarctica preventing the cold water to mix and sink (Kirkman IV & Bitz, 2011), as well as increased sea ice cover and wind-induced sea spray shielding radiation (Hutchinson et al., 2013; Korhonen et al., 2010). The authors stressed that especially changes in wind patterns may have previously contributed to the cooling of waters south of the ACC, but are playing a minor role in present and future changes. Indeed the ozone hole over Antarctica, which has been found to be responsible for this shift in winds, is currently recovering (Banerjee et al., 2020). Along with the surface freshening and decrease in radiation, these effects have been characterized as secondary causes contributing to the delay in Antarctic warming. With the MOC being considered as the primary cause, the authors further predict that the southernmost waters will eventually store some of the excess heat which would result in higher ocean temperatures even south of the ACC (Armour et al., 2016).

Still, there is a large uncertainty in the exact amount of ocean heat changes, which is primarily a result of poor data availability in this relatively remote area of the ocean, where both temperature and salinity data products have so far been scarce due to undersampling (Ishii et al., 2006; Frölicher et al., 2015; Pauthenet et al., 2017; Newman et al., 2019). Recent additions of qualitative data facilitate study investigations of the recent Southern Ocean structure and its responses to the changing climate. The present study contributes to the understanding of how recent temperature and salinity changes affect SLV in the Southern Ocean. All analyses are based on data obtained from the 'GLOBAL-REANALYSIS-PHY-001-031' product provided by the Copernicus Marine Environment Monitoring Service. Here sea surface height (SSH) data from satellite imagery is used, in addition to potential temperature (θ) and practical salinity (S) profiles based on in-situ observations. The θ and S profiles have been approximated into B-spline functions, which allows to apply a functional approach on the spline coefficients to obtain principal components (PCs) (J. Ramsay & Silverman, 2005; Pauthenet et al., 2017). As steric height changes are produced by thermal expansion (raising sea levels) and haline contraction (lowering sea levels) anomalies, the present fPCA captures both contributions at once, instead of analysing temperature and salinity (which are often correlated) separately. The PCs, computed on the entire domain and two sub-domains, form the basis of this study together with steric height values that were computed out of the θ and S data. Both steric height and the PCs have been analysed and related to each other over time from a global, zonal and regional view. Lastly zonal trends of steric height were compared to the total SSH observations from altimetry.

After defining patterns and trends of steric height and the first two modes of the entire Southern Ocean, the subsequent analyses consider interannual trends of the subtropical and the Antarctic sector individually. While the first two main modes of the domain contain the main thermohaline variations over the domain, the temporal

evolution of the modes of the subtropical and the Antarctic sector and their relation to steric height is investigated in more detail.

2 Data and Methods

2.1 Data Sources

The product this study is based on was built from of the four reanalyses GLORYS2V4 from Mercator Ocean, ORAS5 from ECMWF, GloSea5 from Met Office, and C-GLORS05 from CMCC. All four products are 3D gridded descriptions of the physical state of the ocean based on the NEMO model that were processed into an ensemble mean. The extracted data for this project constitutes monthly mean averages from 2008 to 2017 and the horizontal resolution of the grid is 0.25° which has been restricted to every second zonal and meridional grid point (80 × 720 points/profiles). The three variables for this project extracted from GREP are SSH, θ and S. For the following analysis, θ and S data has been restricted to a depth of 2000 m (with 54 depth levels where data is available), where the vast majority of steric height (η) changes take place (Sokolov & Rintoul, 2009; Sutton & Roemmich, 2011; Levitus et al., 2012; Gaillard et al., 2016; Storto et al., 2019).

2.2 B-spline Decomposition

The θ and S profiles have been fitted with a sum of B-spline functions. This step helps to reduce the computational load and to simulate the functional depth-related behaviour of oceanographic properties. The amount of internal knots (K) define the smoothness (and thus the accuracy). Here, each θ or S profile has been decomposed into K=20 B-spline functions. For each of the horizontal stations, the information could therefore be reduced from 54 depth levels for both θ and S variables (2*54 values per profile) to 2*20 eigenfunctions per θ/S profile.

2.3 Functional Principal Component Analysis

Similar to the standard Principal Component Analysis (PCA), the aim of a functional PCA (fPCA) lies in dimensionality reduction and feature extraction. The way it differs from standard PCA is that it is not directly applied on discrete values, but instead on continuous functions fitted on raw data (J. O. Ramsay & Silverman, 2007; Pauthenet et al., 2017). Instead of applying the fPCA on all θ and S values of the 54 depth levels, the modes have been computed on the set of B-spline coefficients.

Before proceeding with the fPCA decomposition, temperature and salinity variables must be non-dimensionalized. Here temperature and salinity anomalies are weighted by the domain-average value of the thermal expansion coefficient (α) and the haline contraction coefficient (β), respectively. Weighted θ and S variables are then normalized by the total buoyancy variance estimated as $var(b) = var(\alpha\theta - \beta S)$. In that way, temperature and salinity are scaled depending on their relative contribution to the variations of buoyancy. For the global domain, α and β values of 1.16×10^{-4} $^{\circ}C^{-1}$ and 7.66×10^{-4} PSU^{-1} were used. In the subtropical and the Antarctic domain the fPCA calculation was based on the respective α and β values of both sectors ($\alpha = 1.73 \times 10^{-4}$ $^{\circ}C^{-1}$ and $\beta = 7.16 \times 10^{-4}$ PSU^{-1} in the subtropical, and $\alpha = 0.58 \times 10^{-4}$ $^{\circ}C^{-1}$ and $\beta = 7.80 \times 10^{-4}$ PSU^{-1} in the Antarctic domain). The fPCA method is then applied on the normalized B-spline coefficients, yielding a set of vertical modes onto which any θ and S vertical profile can be projected (for computational details, see Pauthenet et al. (2017)). A given vertical profile can then be reconstructed as,

$$\theta_j(z) = \bar{\theta}(z) + \sum_{i=1}^{N} y_{i,j}\xi_i^{\theta}(z) \tag{1}$$

$$S_j(z) = \bar{S}(z) + \sum_{i=1}^{N} y_{i,j}\xi_i^{S}(z) \tag{2}$$

.

Here $\bar{\theta}$ and $\bar{S}$ represent the domain-mean reference θ and S profiles, $\xi_i^{\theta}(z)$ and $\xi_i^{S}(z)$ are the temperature and salinity eigenfunctions (also referred to as vertical modes), and $y_{j,i}$ is the mode-i principal component for the vertical profile j. The number N of retained modes defines the order of truncation.

For the entire domain, as well as the subtropical and Antarctic region only, the corresponding principal components have been computed on the monthly climatology of θ and S. On each of the three domains, the first five modes already explain around 99% of the total variance. Here the fPCA provides a set of uncorrelated, time- and space- dependent PC variables that explain the behaviour of the water columns with changing depth with a single value instead of being a function of multiple fixed depth points (J. O. Ramsay & Silverman, 2007; Viviani et al., 2005; Pauthenet et al., 2017).

2.4 Steric Height Computation

Steric height values were computed using the *geo_strf_dyn_height()* function from the Python implementation of The Gibbs SeaWater (GSW) Oceanographic Toolbox. Here it calculates steric height values for each grid point and month out of all monthly temperature and salinity values that are introduced. Beforehand, the temperature and salinity values have been divided by the constant value of gravitational acceleration (9.7963). This study assumes that the majority of steric height changes occur within the first 2000 m and therefore restricts the θ and S data to the provided depth values until 2000 m. The resulting values have been converted into cm as well as zero-centered for presentation and comparison purposes.

3 Results

3.1 Steric Height: Present Distribution and Trends

Mapping the time mean of steric height reveals a continuous north-south gradient in steric height (Figure 1) that is primarily related to the meridional temperature gradient. In order to regionally differentiate between the varying positive and negative trends and their underlying causes, the domain was separated into sectors based on steric height ranges. The superimposed red and blue contour lines organize the study domain into three sectors: The subtropical sector (all steric height values above 40 cm), the Antarctic sector (steric height values below -40 cm) and the subantarctic sector (steric height values in between). Here mainly the subtropical and Antarctic sector are discussed to allow for a clear separation between northern and southern water masses of the Southern Ocean. Figure 1 (lower panel) shows that, apart from the north-south gradient of the time-mean steric height, there are significant regional differences with a general transition from positive trends in the north towards negative trends in the South. Especially in the South Atlantic Ocean, this north-south gradient is clearly visible. In the Indian Ocean such a pattern is also present, but less clear, with deviations south of Australia and near the Agulhas current south-east of Africa, where steric height has decreased over time. From 40°S poleward, the overall trend distribution is very comparable to that of the Atlantic and West Pacific sector. Only in the East Pacific domain, a dominant decrease or increase in steric height along

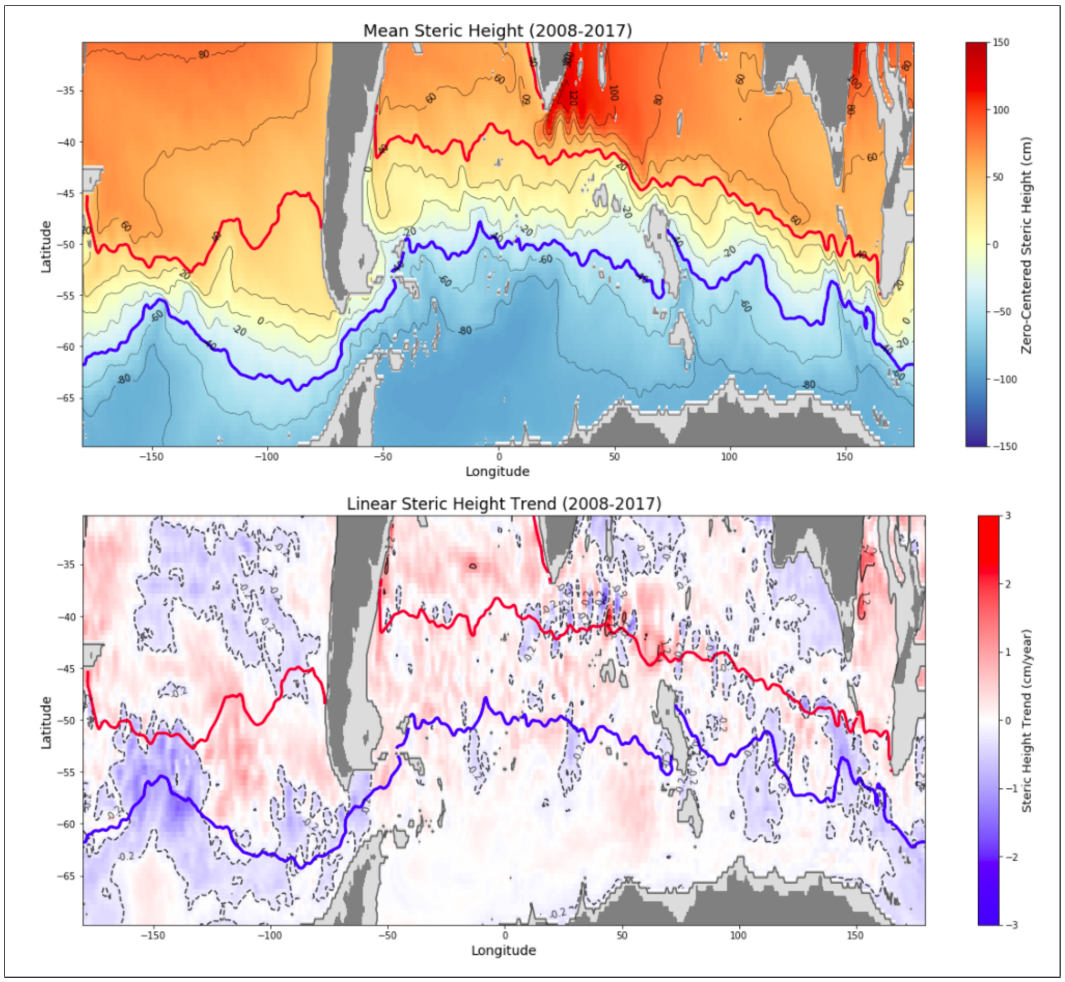

Figure 1. Upper panel: Map of the time-mean zero-centered steric height (0-2000 m) in cm. Lower panel: Map of the linear steric height trend (0-2000 m) in cm. Red contour lines indicate the southern limit of the subtropical sector (η>40 cm) and blue contour lines indicate the northern limit of the Antarctic sector (η<-40 cm) chosen for this study.

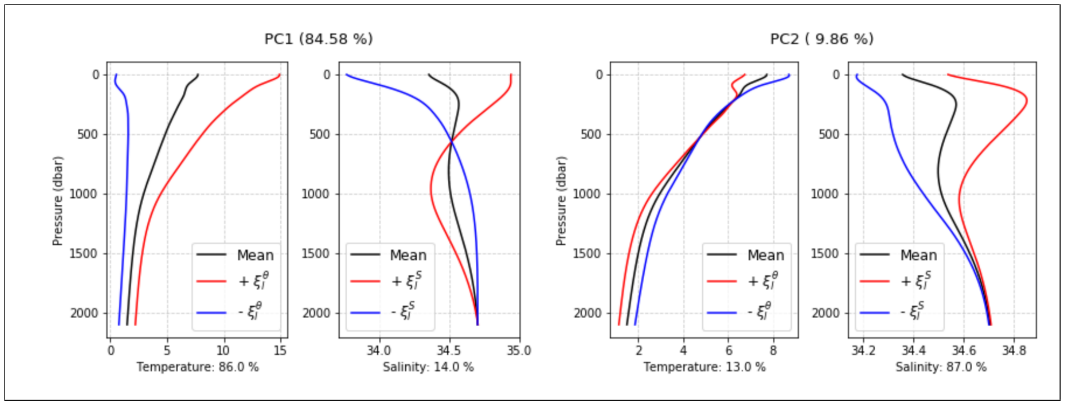

Figure 2. Global domain modes: PC1 and PC2 effect when adding (red curves) and subtracting (blue curves) the eigenfunctions of the mean profiles (black curves) computed from the climatology basis.

the latitudes is not present. Instead, steric height has fallen in the higher and lower latitudes of the study domain and risen in between. In the following these trends are investigated and explained by analyzing variations of the main thermohaline modes of the Southern Ocean.

3.2 Thermohaline Modes and their Relation to Steric Height

This section evaluates the first two modes by analyzing their structure and determining the information contained with higher and lower PC values. The modes themselves do not have dimensions, but each mode conveys information about how θ and S changes with depth. For the purpose of interpreting what higher or lower PC1 and PC2 values reveal about the vertical structure of the water columns, the eigenfunctions ξ_1^θ and ξ_2^S, as calculated by the fPCA, have been added and subtracted to the mean profiles of the modes. Figure 2 illustrates those effects on the first two modes (PC1 and PC2) of the entire domain.

The resulting five thermohaline modes of the Southern Ocean combined explain 99.01% of the θ and S variance. PC1 alone already contains 84.58% of the θ and S variability. The added percentage of explained variance for the higher modes decreases rapidly with each added mode. PC2 explains 9.86% of the averaged θ and S changes, resulting in a combined explained variance of 94.44% of PC1 and PC2 together. The split between the θ and S contribution is shown in Figure 2 just below the vertical profiles. In the case of PC1, θ plays a significantly greater role (86%) than S (14%) in altering the density of the water column, which is why it can be referred to as the thermal mode. The plotted curves in the left panel of Figure 2 reveal that a higher PC1 value represents warmer surface waters for the whole water column (0 to 2000 m), particularly for the surface waters. A lower PC1 value, as represented by the red curve, implies that the temperature is more likely to remain the same with depth and is significantly colder. As for salinity, higher PC1 values indicate saltier surface waters (up to 35 PSU), while a lower value can freshen the surface to almost 33.5 PSU. Further, at around 600 meters below the surface, there is an inversion, meaning that in the intermediate layer salinity decreases when PC1 increases. As temperature greatly dominates this mode, any change in PC1 is more likely to be induced by a change in temperature. Knowing that density decreases with higher temperatures, it can then be concluded that an increase in PC1 is related to an increase in steric height. Due to the dominance of θ this would apply even if there was a similar increase of salinity (which

lowers steric height) over the whole water column. The lack of such a uniform increase or decrease in salinity contributes to the understanding that changes in density are mainly caused by temperature variability.

A large part of the remaining variance is explained by changes in PC2. With only 13% of the variance being explained by temperature changes, salinity dominates the second, haline mode. The right panel of Figure 2 shows that a higher value indicates more saline waters while a lower value indicates fresher waters. This is valid for the entire water column, but is more pronounced in the intermediate waters. Regarding temperature, the effect of adding and subtracting the eigenfunction is mainly impacting the surface waters, with lower temperatures related to a higher PC2 value and vice versa. Due to both the decrease in temperature and increase in salinity a higher PC2 value entails, any increase in PC2 has a negative effect on steric height.

3.3 Spatial Distribution of Modes

There is a clear large scale pattern with higher PC1 values in the subtropical part of the analyzed region and smaller PC1 values closer to the Antarctic continent (Figure 3, upper panel). The higher PC1 values in the north show the north-south temperature gradient of the surface waters that is portrayed in the continuous north-south decline of steric sea level north of the ACC (Figure 1, lower panel). The subtropical surface waters are significantly warmer than the surface waters closer to the South Pole. Roughly the same applies to the salinity, with more saline surface waters in the subtropical regions and fresher waters to the South. Both of these observations are reflected in the effect of one PC unit increase of temperature and salinity respectively to the mean PC1 profile. It is evident that the θ and S gradient in the surface waters from 30°S to around 60°S dominate the overall variability of θ and S.

While PC1 alone explains a substantial part of the variance of temperature and salinity changes, it does not capture the stratification due to salinity and other more complex θ and S structures. South of 50-60°S, the PC1 value remains almost constant and thus does not capture prominent processes in the center and the southern area of the domain that could explain the steric height gradient in the Antarctic sector. The distribution of mean PC2 values over time (Figure 3, lower panel) does reveal gradients both in the subtropical part as well as closer to the pole. Instead of a continuous decrease or increase of PC2 values from north to south, there are noticeably lower PC2 values in the circumpolar region of the ACC region (wide area around 50°S). With the information about what PC2 changes reveal about the vertical structure of the θ and S profiles, it can be concluded that PC2 explains the lower salinity that is characteristic for the ACC area. It is also visible that in contrast to the longitudes of the Atlantic and Indian Ocean sectors, there is a noticeably wider area of lower PC2 values west of the South American continent. This could be attributed to the Humboldt current system transporting cold and fresh surface waters (Silva et al., 2009). The contour lines of PC2 towards the south further reveal the Polar Front (PF) and the Southern Antarctic Circumpolar Front, which could not be identified on the PC1 distribution.

This implies that the first mode is responsible for the steric height drop until roughly 50°S. As the PC1 values farther south have an almost constant value, the subsequent north-south decline in the ACC domain and farther south is a consequence of the salinity gradient captured by the second mode (Figure 3, lower panel). There is a clear gradient in PC2 from south of 50°S until 70°S from fresher to saltier waters, explaining the increase in density towards Antarctica. The increasing values of PC2 are also portraying the colder temperatures at the surface towards the Antarctic coast, as captured by the subservient effect of temperature on PC2 (Figure 2, right panel).

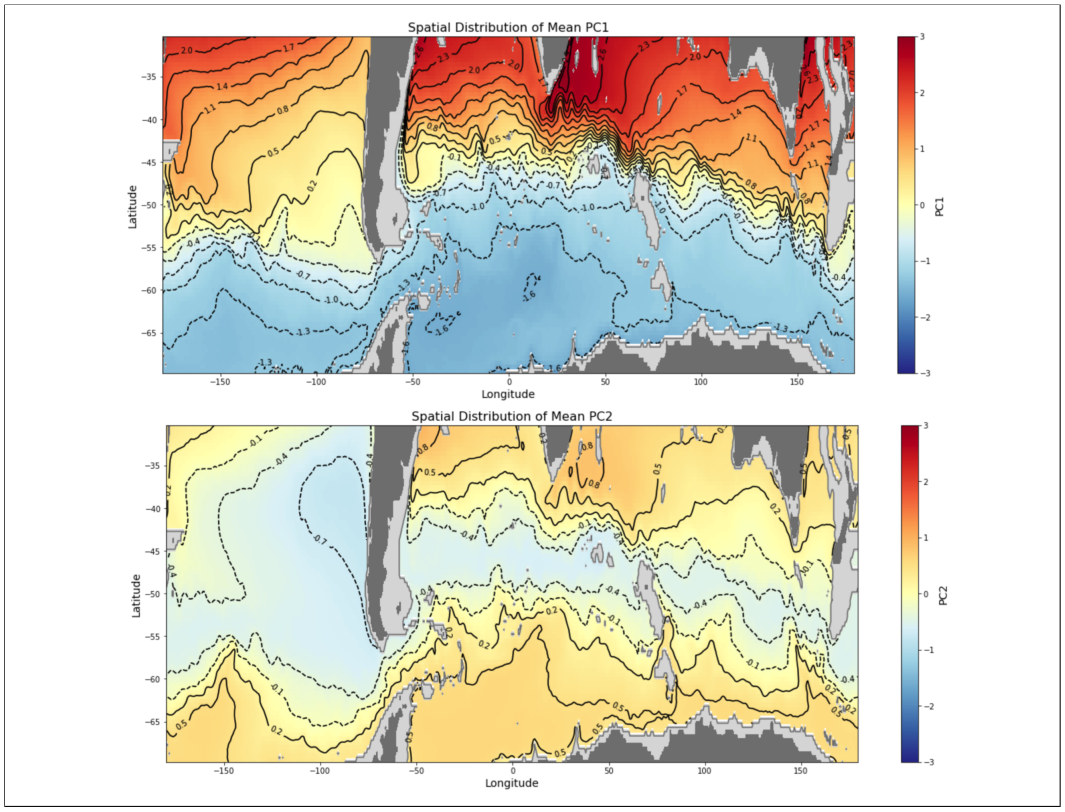

Figure 3. Spatial distribution of the temporal mean (2008 to 2017) of PC1 (upper panel) and PC2 (lower panel) plotted over the entire study domain.

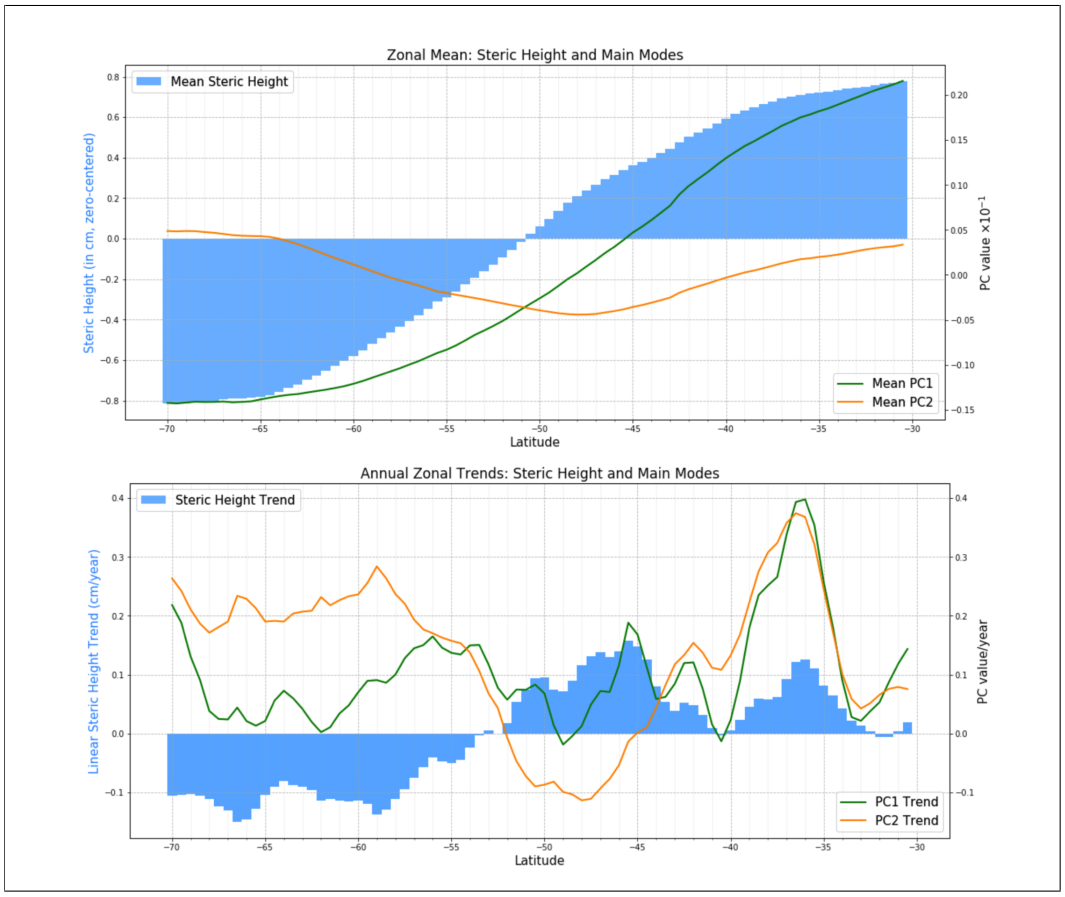

Figure 4. Upper panel: Mean steric height at every 0.5 of latitude from 30°S to 70°S. Mean values of PC1$\times 10^{-1}$ (green) and PC2$\times * 10^{-1}$ (orange) plotted on top. Lower panel: Linear trend slopes of steric height values for every 0.5 of latitude from 30°S to 70°S. Corresponding zonal trends of PC1 (green graph) and PC2 values (orange graph) plotted on top.

3.4 Regional Analysis based on Zonal Means and Trends

Steric height south of 30°S and north of 70°S from 2007 to 2018 has risen 0.44 mm/yr on average, although this trend only follows a moderately accurate linear path. There are also large differences between regions that balance out positive and negative trends. This section analyses zonal means and linear trend slopes, which have been computed for every 0.5 of latitude (Figure 4). It should be stressed that although a clear pattern was discovered, there are also large meridional trend gradients, i.e. differences between the three main basins.

Mapping the spatial distribution of steric height (Figure 1) showed the North-South gradient that is also clearly visible from a zonal mean perspective (Figure 4, upper panel). Steric sea levels at around 30°S are up to 1.6 m higher than those closer to the Antarctic continent. The mean values of the first two modes plotted on top provide a plausible explanation for why the steric height trends are changing between 50°S and 55°S from positive to negative, demonstrated by the zonal trend bars in the lower panel of Figure 4. The mean PC graphs cross each other in this exact zone, indicating that waters south of this zone are dominated by salinity changes, and north of it by temperature changes. It is also in this zone where the mean position of the PF

is located (Kim & Orsi, 2014; Pauthenet et al., 2017, 2019), which could be identified as the southernmost front captured by the mean PC1 map (Figure 1, upper panel). The Polar Frontal Zone between the Subantarctic Front and the PF has previously been identified as the zone where the stratification of the ocean is neither dominated by temperature, nor by salinity (Pollard et al., 2002; Pauthenet et al., 2017). In the lower latitudes it is clear that the rising temperatures have caused rising sea levels, whilst increased salinity in surface and intermediate waters seems to compensate this effect. This compensation is not only derived from the second mode, but is already contained in the first mode itself, with higher values indicating saltier surface waters. However PC1 alone can not explain the negative trend in the south (as even south of the PF it is still mostly positive). Here the haline mode (PC2) dominates density variations and hence has caused lower sea levels as a result of increased salinity. Apart from the PF at around 53°S, there is another close to zero steric height at around 40°S at the Subtropical Front (STF), which separates the significantly warmer subtropical waters from colder waters to the South.

The general north-south trend gradient in steric height is also relevant considering the already prominent zonal decrease of mean steric height values from north to south. The respective trend gradients steepen the slope of higher steric sea levels to the north and lower levels to the South, which thereupon results in a stronger pressure gradient. Such modifications are typically reflected in an intensification of present currents. The ACC is a dominantly wind-driven current that was indeed subject to an increased transport within the last decades, related to the southern annular mode driving stronger westerly winds in recent years (Fyfe et al., 2007; Langlais et al., 2015; Farneti et al., 2015; Liau & Chao, 2017). In the Southern Hemisphere, the strengthening of winds increase the Ekman transport anomaly to the left of the wind direction due to the Coriolis force. It can be expected that the steric effect presented here contributes to the enhanced ACC transport. It is further interesting that the positive trend of PC1 is noticeably greater towards the Antarctic coast.

3.5 PC1 in the Subtropical and Antarctic Sectors

In order to rule out that such results are partly caused by correlation, the fPCA was reapplied separately on the subtropical and the Antarctic sector as defined above. This provides a more detailed picture of the main differences in the general vertical structure and allows to find out whether temperature or salinity (or both) are responsible for the regional steric height trends. The effects of the regional modes are more distinctive of thermohaline characteristics of the two sectors. Hereafter the first mode of the subantarctic domain is called PC1-North and the first mode of the Antarctic domain is referred to as PC1-South.

One foreseeable, but important finding of the regional fPCA computation is that temperature dominates the subtropical (68%), and that salinity dominates the Antarctic density variance (78%). In the subtropical region, computing the modes results in a stronger thermocline as well as warmer mean temperature compared to PC1 with smaller deviations of maximal 2°C (Figure 5, upper panel). In the upper layer, the effect with one added eigenfunction remains similar, so that higher values of the first mode are again indicative of warmer and saltier waters. Salinity changes primarily occur at the surface, where warmer waters farther north equal saltier waters. In comparison to the first mode of the entire domain (PC1), there is a low mean salinity at about 1000 m depth, representing the Antarctic Intermediate Waters between the saltier Subantarctic Mode Water and the Upper Circumpolar Deep Water. The boundary to the subantarctic waters is too far south for PC1-North to depict the salinity inversion from before (Figure 2, right panel). The net effect on steric height is therefore less strong, since salinity compensates the decrease in density caused by higher temperatures in the whole water column. Salinity changes are now slightly dominant

(54%) which is a result of a much smaller range of temperatures. The T-S percentages here are based on the same $\alpha - \beta$ ratio as calculated from the entire domain to allow a more homogeneous interpretation. Here the mean θ and S values are both significantly affecting density by offsetting each other, although the temperature gradient prevails in accounting for the steric height gradient from north to south.

In the Antarctic sector, the mean profile of PC1-South (grey temperature curve of PC1-South in Figure 5) describes the temperature effect covered by higher values of PC2 in the global domain (see Figure 2, right panel, and Figure 5, lower panel). PC1-South captures the characteristics of polar waters of having a much smaller range of temperatures, a shallow thermocline and a more distinctive mixed layer. Higher values are associated with an increase in temperature at all vertical levels (until 2000 m). As for salinity, higher PC1-South values indicate fresher waters until 800 m below which they are slightly more salty. Temperature and salinity both significantly impact the density of the water column. The effect that this mode induces on steric height is positive, which is lightly noticeable in Figure 2, where there is a zonal steric height gradient from north to south, even if less apparent than at lower latitudes. While the global fPCA revealed the main characteristics of the Southern Ocean, these two local modes allow a more reliable conclusion on why steric height has risen or fallen over the years depending on the region.

3.6 Effect of PC1, PC1-North and PC1-South on steric height

Any change in steric height is a result of variations in both temperature and salinity. Therefore, steric height changes can be approximately quantified using PC1 variations for any given domain as long as the first mode captures a sufficiently large fraction of the total variance. This is the case for the three domains under consideration (global: 85%, subtropical: 74%, and Antarctic: 77%). In that case, the domain-averaged change in steric height due to temperature and salinity, respectively, is proportional to the depth-mean of the associated vertical mode times the mean PC1 change (see Table 1),

$$\Delta\eta \simeq \Delta\eta_\theta + \Delta\eta_S, \tag{3}$$

with $\Delta\eta_\theta = \alpha H \overline{\xi_1^\theta} \Delta y_1$ and $\Delta\eta_S = -\beta H \overline{\xi_1^S} \Delta y_1$ the thermosteric and halosteric domain-averaged contributions driven by variations in PC1, respectively. Here, H is the total depth of considered profiles (here $H = 2000m$), $\overline{\xi_1^\theta}$ and $\overline{\xi_1^S}$ the depth-averaged vertical modes associated with PC1, and Δy_1 the domain-averaged change of PC1. These estimates are only approximate in so far as the α and β coefficients are not constant in the ocean. However, their relative variations are sufficiently small in each sub-region to yield the correct sign and magnitude of the steric height contributions.

A unit increase of the first global mode (PC1) results in a significant warming and therefore raises steric height by 69 cm which is only slightly damped by salinity (-2 cm), resulting in a net rise of 67 cm. This first global mode is able to capture the most prominent features, but is less useful in explaining more local and complex Southern Ocean water characteristics. Here the regional modes allow for a more detailed analysis of the different structures and interannual trends. The addition of one unit to the subtropical mode (PC1-North) induces a steric height rise of 10 cm (greatly compensated by salinity), while the positive effects induced by temperature and salinity with an increase of one PC1-South unit increases steric height by 11 cm (Table 1).

An approximation of a spatial mean linear trend of each domain can be achieved by multiplying the linear PC trends with the respective steric height increase per PC unit ('Net $\Delta\eta/\Delta y_1$' in Table 1). For the global domain, the mean increase of $7.22{*}10^{-3}$/yr would increase the steric sea level in the Southern Ocean by 0.48 mm/yr,

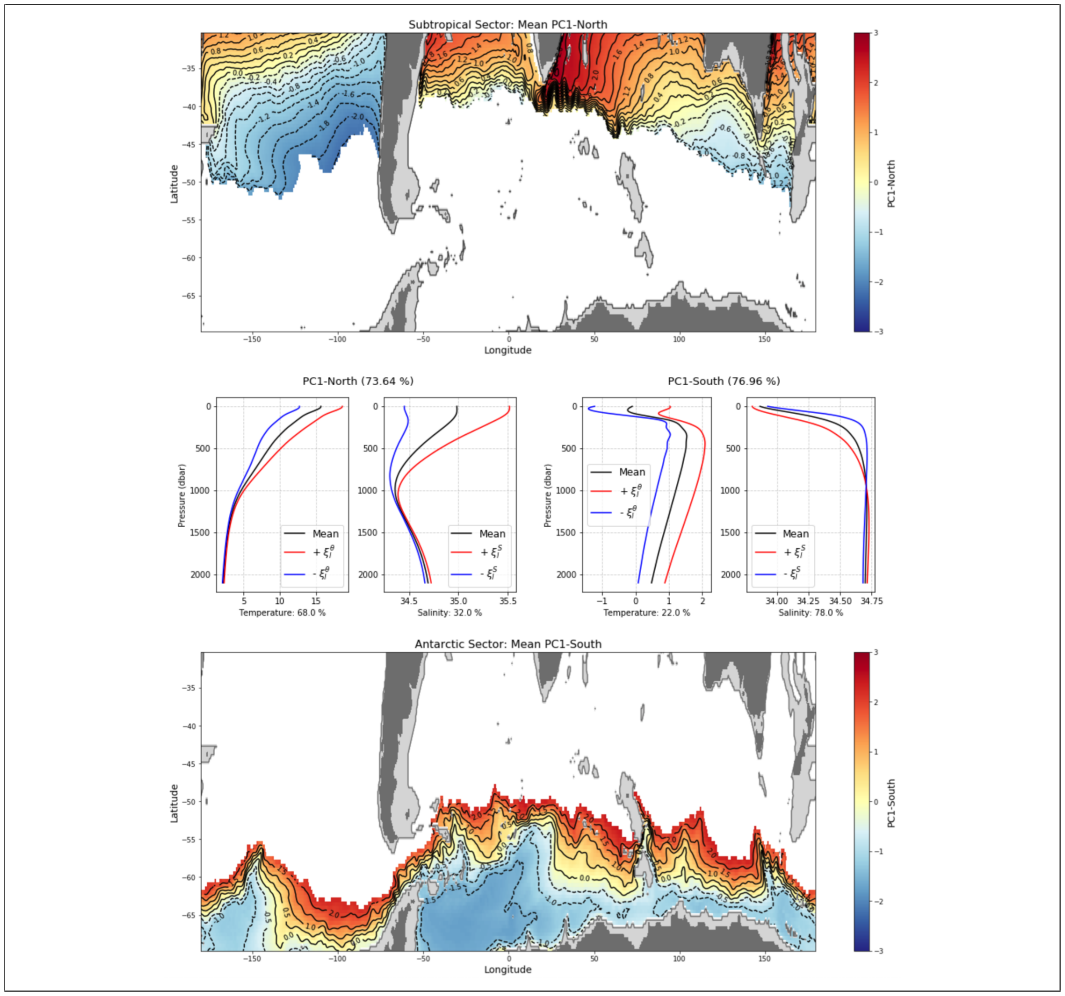

Figure 5. Spatial distribution of the temporal mean (2008-2017) of the PC1-North (upper panel) and PC1-South (lower panel) domain with dashed lines indicating negative values. Profile plots in the central panel show the respective effect on PC1-North and PC1-South when adding (red curves) and subtracting (blue curves) the eigenfunctions of the respective mean profiles (black curves).

Table 1. Thermal expansion and haline contraction coefficients of the respective domains, along with the θ and S effects the first modes of each region induce on steric height with one added eigenfunction.

	Global Domain (PC1)	Subtropical Domain (PC1-North)	Antarctic Domain (PC1-South)
α ($^\circ C^{-1}$)	1.16 $\times 10^{-4}$	1.73×10^{-4}	0.58×10^{-4}
β (PSU^{-1})	7.66 $\times 10^{-4}$	7.16×10^{-4}	7.80×10^{-4}
$\overline{\xi_1^\theta}$ ($^\circ$C)	+2.89	+0.83	+0.54
$\overline{\xi_1^S}$ (PSU)	+0.01	+0.13	-0.03
$\Delta\eta_\theta/\Delta y_1$ (cm/PC)	+69	+29	+6
$\Delta\eta_S/\Delta y_1$ (cm/PC)	-2	-19	+5
Net $\Delta\eta/\Delta y_1$ (cm/PC)	+67	+10	+11

which is very close to the actual trend of 0.44 mm/yr. Applying this approach in the two sub-domains, the predicted linear trends results in an annual rise of 0.72 mm/yr (vs. actual: 0.87 mm/yr) in the subtropical, and a fall of 0.70 mm/yr (vs. actual: -0.44 mm/yr) in the Antarctic domain.

Comparing the spatial trend distribution of steric height with that of PC1-North and PC1-South (Figure 6) hints to causes for the divergent regional trends. In the subtropical sector of the East Pacific, where steric height variations are mainly dependent on temperature changes, steric height has dropped due to low PC1-North values primarily indicating colder temperatures (except for waters close to the South American coastline). The Amundsen Sea has experienced decreasing temperatures as well, along with an increase in sea surface salinity (negative PC1-South trend). Those temperature and salinity trends are responsible for the differing trends visible in the East Pacific sector. As for the West Pacific sector and the Indian and Atlantic domains, the PC1-North trends dominantly suggest that the subtropical domain waters have become significantly warmer and saltier. The model θ and S data (54 levels averaged from 0 to 2000 m) validate this information stored in the PCs. The upper panels of Figure 7 show that the positive steric height trend in the subtropical domain does mainly arise from rising temperatures, as salinity has significantly increased in most regions, lowering sea levels. Despite increased salinity and the fact that the temperature trend is not spatially consistent north of the PF and actually negative in several northern areas, the dominant positive trend of temperature has caused the subtropical increase in steric height. This finding stresses the idea that temperature has a much greater influence on SLV compared to salinity in the northern waters of the Southern Ocean.

Antarctic waters have instead become mostly colder and saltier at the surface (negative PC1-South trends, Figure 6, lower panel). Here the model data of θ and S confirm that salinity dominates the steric height evolution in very high-latitude waters. Even though temperatures have mostly risen below 65°S and partly farther north, steric height has dropped as a result of the significant increase in salinity in almost

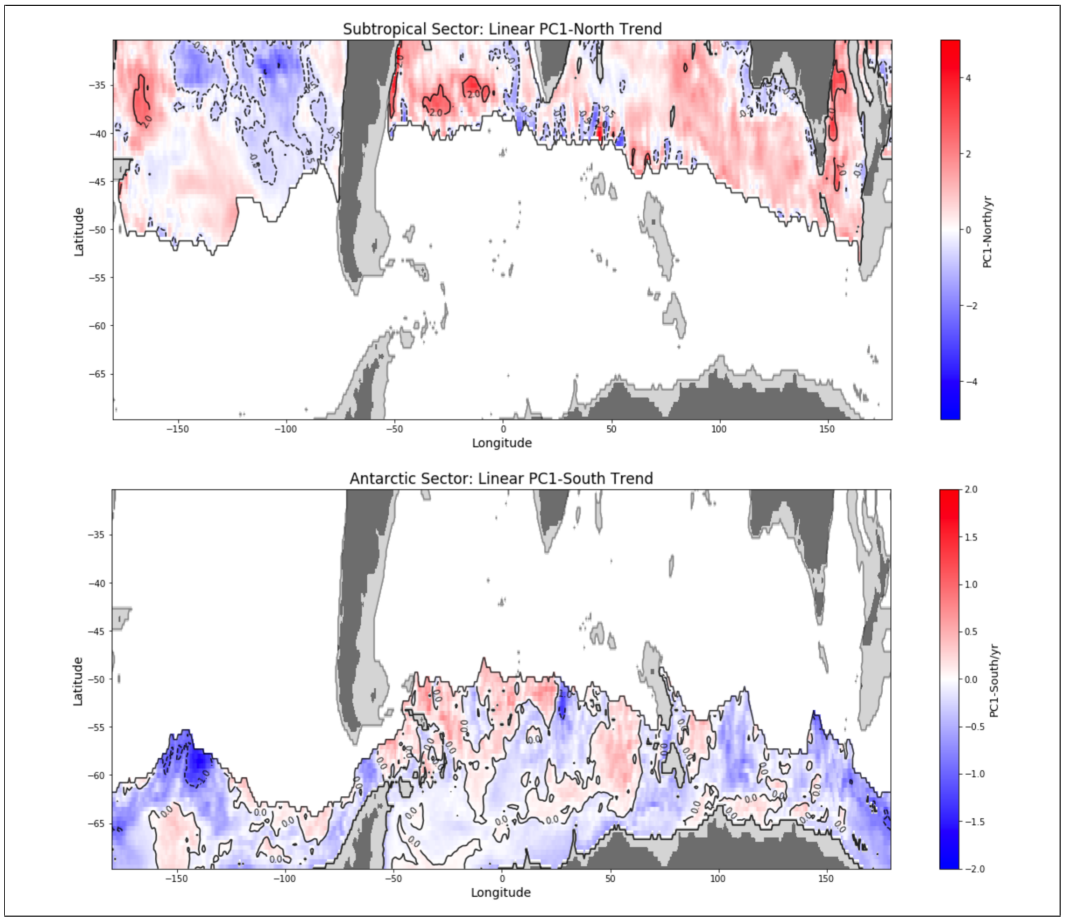

Figure 6. Map of the linear trends of the subtropical and Antarctic mode represented by the linear slope through time (from 2008 to 2017) on all grid points.

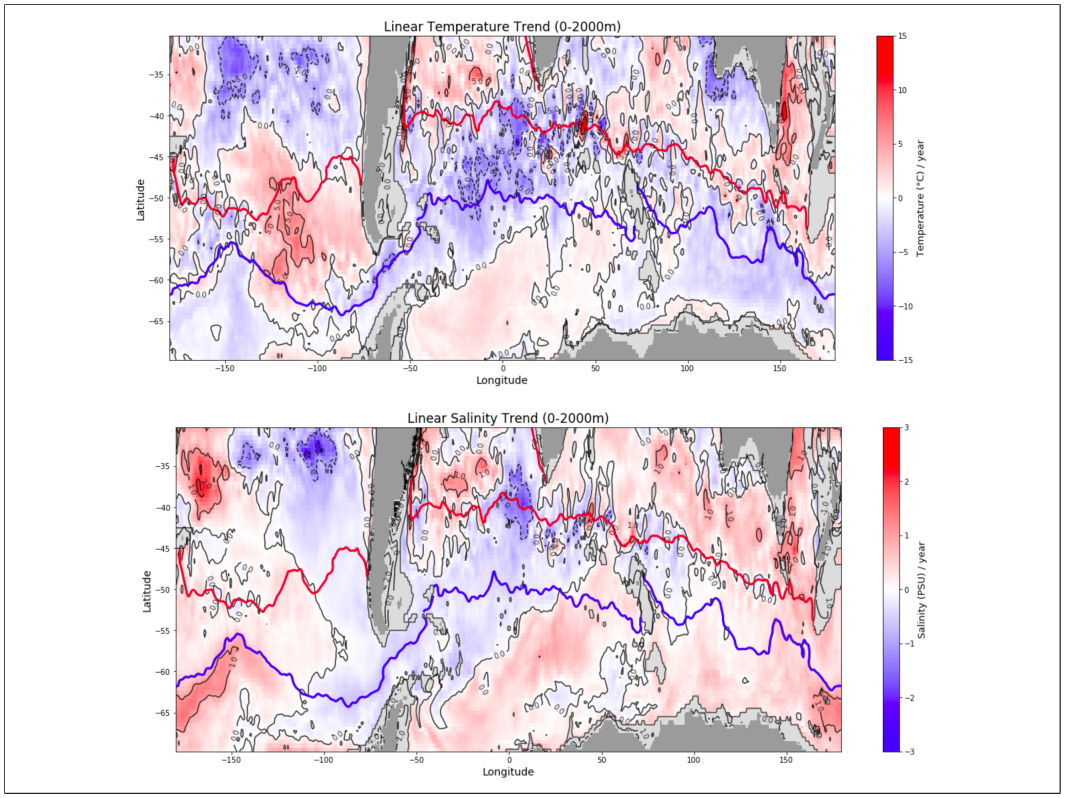

Figure 7. Maps of the linear trends of the model temperature (upper panel) and salinity (lower panel) as means of the upper 2000 m water column, represented by the linear slope through time (from 2008 to 2017) on all grid points.

all Antarctic regions apart from the area near the Drake Passage (Figure 7, lower left panel). These results also explain the strikingly high PC1 values that were found closer to the Antarctic coast (Figure 4, lower panel) caused by warmer waters near the Antarctic coastline. However in the more southern sector of the ACC and most high-latitude areas in the Indian and West Pacific domain temperatures have noticeably dropped. As for the positive salinity trend, the Antarctic mode PC1-South further reveals that waters have mostly become more saline at the surface and intermediate layers instead of below 1000 m (Figure 5, central panel on the very right). The warmer and saltier waters closer to the Antarctic coast, and colder and partly fresher waters at around 50°S to 60° support the suggestion from Armour et al. (2016) with the MOC being the main driver of the cooling trend. They also fit into the picture of a strengthening of the ACC, in that the MOC lets warm and salty water masses from the deep ocean come to the surface close to Antarctica, from where the circulation transports colder and less saline surface waters north to the ACC subduction zone.

The negative PC1-South and the positive PC1-North trends display on the steric height trends (Figure 1, lower panel), raising sea levels north of the ACC and mainly lowering sea levels close to the Antarctic coast. Exceptions such as colder waters (negative PC1-North trends) south of Australia or fresher waters (positive PC1-South trends) between 50°S and 55°S in the Atlantic domain have produced opposed steric sea level trends in those regions. Although there are distinct exceptions apparent and it is thus necessary to further analyze such differences in more regional contexts, it is reasonable to distinguish between mostly rising steric sea levels in the subtropical, and

falling steric sea levels in the Antarctic domain (as demonstrated by the zonal mean trends in Figure 4).

3.7 Non-linear Trend Variations: Subtropical and Antarctic Sector

As shown in Figure 4, PC1 and PC2 trends have indicated rising temperatures and increased salinity at almost all latitudinal ranges and vertical ranges of the water column, while steric height has risen in the subtropical and fallen in the Antarctic sector. Figure 8 shows the non-seasonal time series of steric height and the predicted non-seasonal time series of steric height based on PC1-North and PC1-South respectively, for which all PC1-North and PC1-South values have been detrended and multiplied by their regression coefficient (9.24 for PC1-North and 12.04 for PC1-South). In the Antarctic sector, the predicted data follows the actual steric height course reasonably well, while in the subtropical domain the θ and S data is possibly less homogeneous which flattens the predicted steric height. The positive steric height trend in the subtropical sector is primarily arising from a non-consistent increase from 2010 until 2014. From 2014, the monthly data outline a consistent decline in steric sea level until the beginning of 2017, reducing the linear trend to 0.9 mm/yr. From 2008 to 2017, this still signifies a trend of almost 1 cm per decade. In the Antarctic sector, the steric height results show falling sea levels from 2014 to 2016. Interestingly, both model simulations and observations have shown that the sea ice area (SIA) around Antarctica has decreased significantly since 2014, after a continuous increase in the past decades (Pu et al., 2020). Those two trends could be related to each other, as the former freshening of the Southern Ocean has been related to a northward sea ice transport introducing fresher waters farther north (Haumann et al., 2016). Following Haumann et al. (2020), the latest decrease in SIA could have caused an increase in salinity in addition to relatively colder subsurface waters as a result of a weakened stratification. This increase in salt content along with the decrease in subsurface temperature could have caused the present decline in steric height after 2014. On average, the negative trend of steric height in the southernmost waters of the Southern Ocean predicts an annual fall in steric height of -0.4 mm/yr.

The respective non-seasonal time series of PC1-North and PC1-South are shown in Figure 9. As both modes have a negative effect on density and a positive effect on steric sea level, their time series are essentially following a similar course to those of the estimated trends (Predicted η in Figure 8). Comparing the two regional modes with PC1 and PC2 of the entire domain reveals that in the subtropical domain subtropical waters have indeed gotten both warmer and saltier as suggested by the zonal trends of the first two modes in the global domain. In the Antarctic domain however, the negative trend in PC1-South indicates colder and saltier waters above 800 m depth, instead of warmer waters as could be presumed by the positive PC1 trends. Apart from correlation, those positive PC1 trends were likely a result of the salinity effect this mode captures, as higher PC1 values indicate saltier surface and fresher intermediate waters. This is a similar effect to that of decreasing PC1-South values, and could certainly be indicating increased upwelling of salty waters in the southernmost region. It should be noted that the results of the Antarctic domain are based on relatively poor observations (Sallée, 2018), which explains that there are only few studies, especially on high-latitude salinity trends. The positive temperature trends north of the ACC and the negative temperature trends in Antarctic waters however are in agreement with recent observation-based studies from Armour et al. (2016) and Auger et al. (2021).

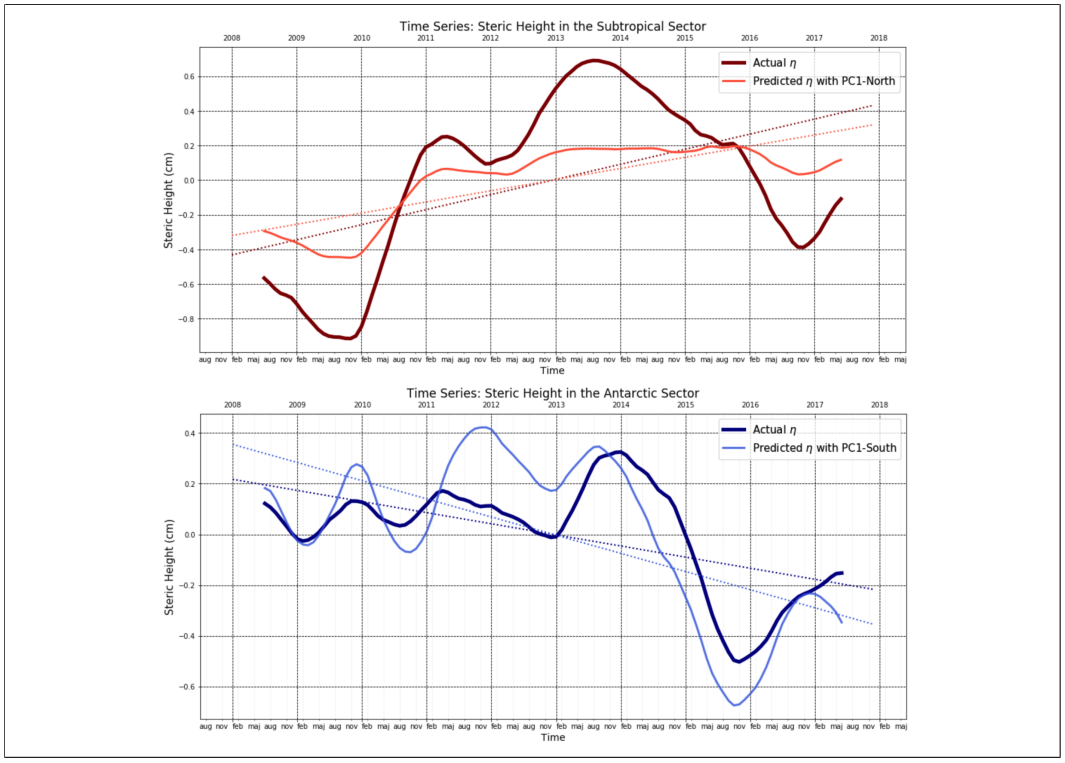

Figure 8. Non-seasonal time series of actual and predicted time series of steric height in the subtropical (upper panel) and the Antarctic (lower panel) sector from 2008 to 2017. Predictive time series after a linear regression model where steric height is based on PC1-North and PC1-South values. Dotted lines represent the linear trends of the subtropical (Actual = 0.870 mm/yr; Predicted = 0.644 mm/yr) and the Antarctic (Actual = -0.438 mm/yr; Predicted = -0.717 mm/yr) sector.

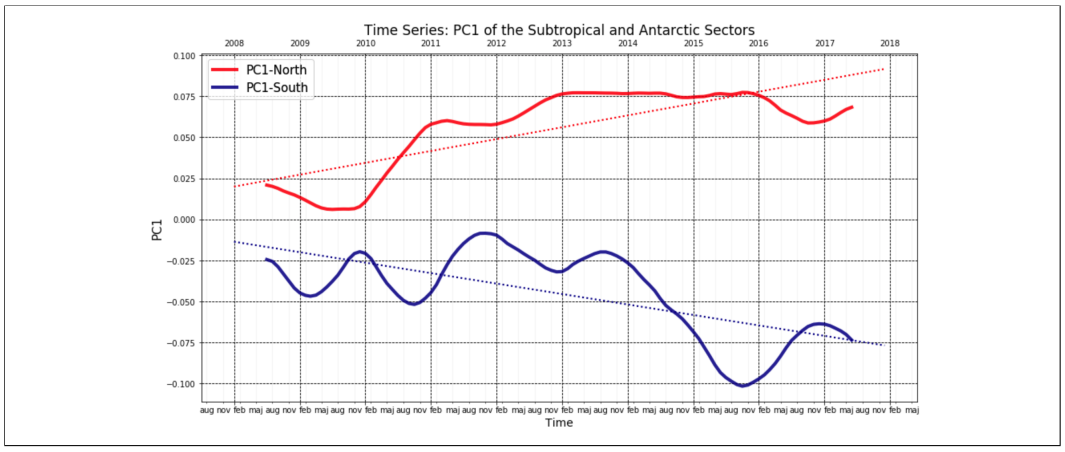

Figure 9. Non-seasonal time series of PC1 computed individually for the subtropical (red) and the Antarctic (blue) sector from 2008 to 2017. Dotted graphs show linear trends (PC1-North: $7.22 * 10^{-3}$/yr; PC1-South: $-6.37 * 10^{-3}$/yr).

4 Conclusions

In the present study temperature and salinity variations were related to steric height changes in the Southern Ocean. The originality of the analysis was to first decompose the θ and S profiles into vertical thermohaline modes and to then compare the spatiotemporal evolution of the main modes with sea level variations. To generalize, the temporal analysis suggests that the salt content of the Southern Ocean's surface and intermediate layer has increased north and south of the ACC. Further the results indicate that only Antarctic waters below 800 m depth and in the Atlantic basin have experienced minor freshening (the subantarctic domain was not in the focus of this study). In the subtropical sector, especially just north of the STF (35°S to 40°S), surface and intermediate waters have become warmer and saltier. As suggested by previous studies, the cooling of Antarctic waters from the surface up to 2000 m depth could also be identified, along with a warming trend in various regions closer to the Antarctic coast which can be associated with enhanced upwelling of deeper mater masses (Goosse et al., 2004; Li et al., 2013; Sallée et al., 2013; Armour et al., 2016). There are regional disparities at nearly all zonal ranges, but the overall trend points towards warmer and saltier subtropical, and colder and saltier (upper layer) or fresher (lower intermediate layer) waters closer to Antarctica. Higher temperatures north of the ACC portray increased oceanic heat storage from atmospheric warming, however more data over longer timescales are needed to define more certain results.

Despite the large-scale increase in salinity, the average annual trend of steric height in the Southern Ocean has increased compared to previous studies providing steric height estimations until 2015 (Ishii et al., 2006; von Schuckmann et al., 2010; Wang et al., 2017; Storto et al., 2019). In the subtropical waters of the Southern Ocean, temperature dominates the present structure of steric height, accounting for its mean distribution and its positive trend. However despite higher temperatures in this region, the thermosteric contribution has partly been offset by a non-uniform spatial pattern of increased salinity. While in other oceans, steric height variability is largely controlled by temperature alone, salinity changes in the Southern Ocean are significantly damping the thermosteric effect of higher temperatures north of the ACC and are the dominant reason for negative steric height trends south of the ACC, where they reinforce the thermosteric effect of mostly colder waters. If these trends continue, the prominent sea level slope from north to south will further steepen which might in turn carry on altering ocean dynamics.

By encoding the leading structure of oceanographic profiles, vertical modes serve to accurately describe not only the present or historic condition and mean distribution of such properties, but can further be used to monitor present changes in a functional and objective way. The present study showed that the first two modes (PC1 and PC2) of the Southern Ocean can be generalized into the thermal mode in the north and the haline mode in the south (Pauthenet et al., 2017, 2019). Especially towards the higher latitudes, steric height variability does not project distinctly on these modes due to the diversity of water masses south of 30°S. Applying the fPCA on two sub-regions (PC1-North and PC1-South) allowed to clarify the contrasting development in steric height trends in the subtropical and the Antarctic sector. The time period of this study is too short, however, to draw confident conclusions about the long-term climate trends, but serves to investigate intradecadal processes that can deviate from more linear long-term trends.

To put the steric height results into perspective with the total sea level trend, the mean linear steric height trend can be subtracted from the altimetry-based SSH data, and the zonal steric trends can be evaluated relative to zonal SSH trends (Figure 10). Total SSH has increased at all latitudes, at a rate of 0.07 cm/yr at 67°S to 0.5 cm/yr at 45°S. From 2008 to 2017, the reanalysis data suggests that the total sea level of the Southern Ocean (30°S to 70°S) has risen by 3.1 cm, of which 14% (0.44

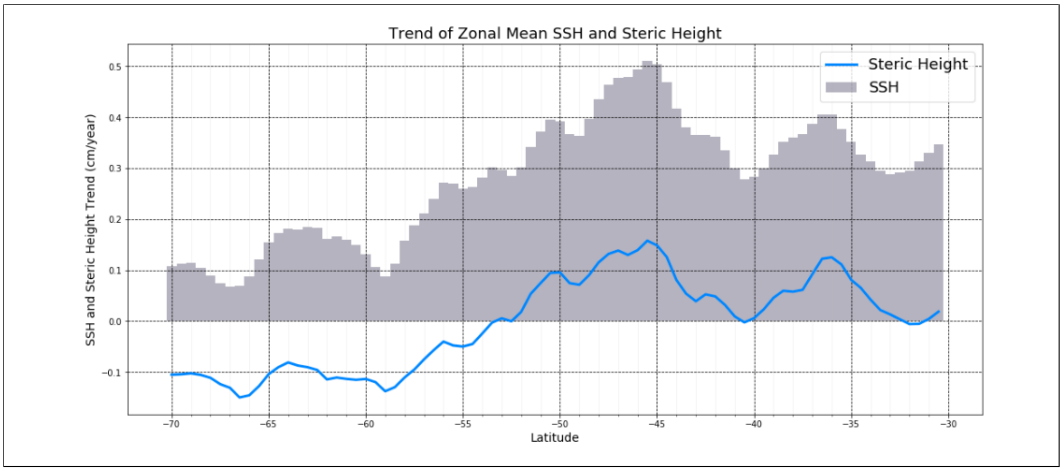

Figure 10. Linear trend slopes of steric height (blue graph) and SSH (grey bars) for every 0.5 of latitude from 30°S to 70°S, based on zonal means from 2008 to 2017.

cm) were attributed to an increase in the net thermosteric sea level. SSH in the subtropical sector showed an increase in 3.8 cm, while sea level in the Antarctic sector has only risen by 1.3 cm due to the significant compensation caused by the halosteric contribution. Despite of an average increase of Southern Ocean steric height trends compared to previous studies (Ishii et al., 2006; von Schuckmann et al., 2010; Wang et al., 2017; Storto et al., 2019), the relative steric contribution has decreased, which is likely due to accelerated melting of ice sheets and glaciers. The barystatic contribution significantly enhances the present and near future SLR of Southern Ocean waters. At the same time, this study showed that steric height defines spatial patterns and can strongly influence the magnitude of recent sea level changes. The almost uniform increase in non-steric sea levels has outweighed the steric sea level fall south of the PF and reinforced higher sea levels caused by ocean warming in higher latitudes. In other words, the thermo- and halosteric contributions have damped the barystatic SLR in Antarctic waters and significantly contributed to the SLR in subtropical waters of the Southern Ocean.

Acknowledgments

Part of this work was carried out at the University of Gothenburg as a Master's thesis project under the supervision of Fabien Roquet.

The 'GLOBAL-REANALYSIS-PHY-001- 031' product was provided by the Copernicus Marine Environment Monitoring Service.

References

Armour, K. C., Marshall, J., Scott, J. R., Donohoe, A., & Newsom, E. R. (2016). Southern ocean warming delayed by circumpolar upwelling and equatorward transport. *Nature Geoscience*, *9*(7), 549–554.

Auger, M., Morrow, R., Kestenare, E., Sallée, J.-B., & Cowley, R. (2021). Southern ocean in-situ temperature trends over 25 years emerge from interannual variability. *Nature Communications*, *12*(1), 1–9.

Banerjee, A., Fyfe, J. C., Polvani, L. M., Waugh, D., & Chang, K.-L. (2020). A pause in southern hemisphere circulation trends due to the montreal protocol.

Nature, *579*(7800), 544–548.

Cheng, L., Abraham, J., Zhu, J., Trenberth, K. E., Fasullo, J., Boyer, T., ... others (2020). *Record-setting ocean warmth continued in 2019.* Springer.

Farneti, R., Downes, S. M., Griffies, S. M., Marsland, S. J., Behrens, E., Bentsen, M., ... others (2015). An assessment of antarctic circumpolar current and southern ocean meridional overturning circulation during 1958–2007 in a suite of interannual core-ii simulations. *Ocean Modelling*, *93*, 84–120.

Frölicher, T. L., Sarmiento, J. L., Paynter, D. J., Dunne, J. P., Krastingfstort, J. P., & Winton, M. (2015). Dominance of the southern ocean in anthropogenic carbon and heat uptake in cmip5 models. *Journal of Climate*, *28*(2), 862–886.

Fyfe, J. C., Saenko, O. A., Zickfeld, K., Eby, M., & Weaver, A. J. (2007). The role of poleward-intensifying winds on southern ocean warming. *Journal of Climate*, *20*(21), 5391–5400.

Gaillard, F., Reynaud, T., Thierry, V., Kolodziejczyk, N., & Von Schuckmann, K. (2016). In situ–based reanalysis of the global ocean temperature and salinity with isas: Variability of the heat content and steric height. *Journal of Climate*, *29*(4), 1305–1323.

Goosse, H., Masson-Delmotte, V., Renssen, H., Delmotte, M., Fichefet, T., Morgan, V., ... Stenni, B. (2004). A late medieval warm period in the southern ocean as a delayed response to external forcing? *Geophysical Research Letters*, *31*(6).

Haumann, F. A., Gruber, N., & Münnich, M. (2020). Sea-ice induced southern ocean subsurface warming and surface cooling in a warming climate. *AGU Advances*, *1*(2), e2019AV000132.

Haumann, F. A., Gruber, N., Münnich, M., Frenger, I., & Kern, S. (2016). Sea-ice transport driving southern ocean salinity and its recent trends. *Nature*, *537*(7618), 89–92.

Hutchinson, D. K., England, M. H., Santoso, A., & Hogg, A. M. (2013). Interhemispheric asymmetry in transient global warming: The role of drake passage. *Geophysical Research Letters*, *40*(8), 1587–1593.

Ishii, M., Kimoto, M., Sakamoto, K., & Iwasaki, S.-I. (2006). Steric sea level changes estimated from historical ocean subsurface temperature and salinity analyses. *Journal of oceanography*, *62*(2), 155–170.

Kim, Y. S., & Orsi, A. H. (2014). On the variability of antarctic circumpolar current fronts inferred from 1992–2011 altimetry. *Journal of Physical Oceanography*, *44*(12), 3054–3071.

Kirkman IV, C. H., & Bitz, C. M. (2011). The effect of the sea ice freshwater flux on southern ocean temperatures in ccsm3: Deep-ocean warming and delayed surface warming. *Journal of Climate*, *24*(9), 2224–2237.

Korhonen, H., Carslaw, K. S., Forster, P. M., Mikkonen, S., Gordon, N. D., & Kokkola, H. (2010). Aerosol climate feedback due to decadal increases in southern hemisphere wind speeds. *Geophysical Research Letters*, *37*(2).

Langlais, C. E., Rintoul, S. R., & Zika, J. D. (2015). Sensitivity of antarctic circumpolar current transport and eddy activity to wind patterns in the southern ocean. *Journal of Physical Oceanography*, *45*(4), 1051–1067.

Levitus, S., Antonov, J. I., Boyer, T. P., Baranova, O. K., Garcia, H. E., Locarnini, R. A., ... others (2012). World ocean heat content and thermosteric sea level change (0-2000 m), 1955–2010. *Geophysical Research Letters*, *39*(10).

Li, C., von Storch, J.-S., & Marotzke, J. (2013). Deep-ocean heat uptake and equilibrium climate response. *Climate Dynamics*, *40*(5-6), 1071–1086.

Liau, J.-R., & Chao, B. F. (2017). Variation of antarctic circumpolar current and its intensification in relation to the southern annular mode detected in the time-variable gravity signals by grace satellite. *Earth, Planets and Space*, *69*(1), 93.

Meredith, M., Sommerkorn, M., Cassotta, S., Derksen, C., Ekaykin, A., Hollowed,

A., ... others (2019). Chapter 3: Polar regions.
Newman, L., Heil, P., Trebilco, R., Katsumata, K., Constable, A., van Wijk, E., ... others (2019). Delivering sustained, coordinated, and integrated observations of the southern ocean for global impact. *Frontiers in Marine Science*, *6*, 433.
Oke, P. R., & England, M. H. (2004). Oceanic response to changes in the latitude of the southern hemisphere subpolar westerly winds. *Journal of Climate*, *17*(5), 1040–1054.
Pauthenet, E., Roquet, F., Madec, G., & Nerini, D. (2017). A linear decomposition of the southern ocean thermohaline structure. *Journal of Physical Oceanography*, *47*(1), 29–47.
Pauthenet, E., Roquet, F., Madec, G., Sallée, J.-B., & Nerini, D. (2019). The thermohaline modes of the global ocean. *Journal of Physical Oceanography*, *49*(10), 2535–2552.
Pollard, R., Lucas, M., & Read, J. (2002). Physical controls on biogeochemical zonation in the southern ocean. *Deep Sea Research Part II: Topical Studies in Oceanography*, *49*(16), 3289–3305.
Pu, Y., Liu, H., Yan, R., Yang, H., Xia, K., Li, Y., ... others (2020). Cas fgoals-g3 model datasets for the cmip6 scenario model intercomparison project (scenariomip). *Advances in Atmospheric Sciences*, *37*(10), 1081–1092.
Ramsay, J., & Silverman, B. (2005). Principal components analysis for functional data. *Functional data analysis*, 147–172.
Ramsay, J. O., & Silverman, B. W. (2007). *Applied functional data analysis: methods and case studies*. Springer.
Sallée, J.-B. (2018). Southern ocean warming. *Oceanography*, *31*(2), 52–62.
Sallée, J.-B., Shuckburgh, E., Bruneau, N., Meijers, A. J., Bracegirdle, T. J., & Wang, Z. (2013). Assessment of southern ocean mixed-layer depths in cmip5 models: Historical bias and forcing response. *Journal of Geophysical Research: Oceans*, *118*(4), 1845–1862.
Shi, J.-R., Xie, S.-P., & Talley, L. D. (2018). Evolving relative importance of the southern ocean and north atlantic in anthropogenic ocean heat uptake. *Journal of Climate*, *31*(18), 7459–7479.
Silva, N., Rojas, N., & Fedele, A. (2009). Water masses in the humboldt current system: Properties, distribution, and the nitrate deficit as a chemical water mass tracer for equatorial subsurface water off chile. *Deep Sea Research Part II: Topical Studies in Oceanography*, *56*(16), 1004–1020.
Sokolov, S., & Rintoul, S. R. (2009). Circumpolar structure and distribution of the antarctic circumpolar current fronts: 2. variability and relationship to sea surface height. *Journal of Geophysical Research: Oceans*, *114*(C11).
Storto, A., Bonaduce, A., Feng, X., & Yang, C. (2019). Steric sea level changes from ocean reanalyses at global and regional scales. *Water*, *11*(10), 1987.
Sutton, P., & Roemmich, D. (2011). Decadal steric and sea surface height changes in the southern hemisphere. *Geophysical research letters*, *38*(8).
Viviani, R., Grön, G., & Spitzer, M. (2005). Functional principal component analysis of fmri data. *Human brain mapping*, *24*(2), 109–129.
von Schuckmann, K., Speich, S., Gaillard, F., & Le Traon, P.-Y. (2010). Large regional contributions of ocean heat content variability, freshwater content and steric height changes. *EGUGA*, 11888.
Wang, G., Cheng, L., Boyer, T., & Li, C. (2017). Halosteric sea level changes during the argo era. *Water*, *9*(7), 484.